# Generalized Lenard-Balescu calculations of electron-ion temperature relaxation in beryllium plasma

Zhen-Guo Fu,[1,2] Zhigang Wang,[2] Da-Fang Li,[2] Wei Kang,[3] and Ping Zhang[1,2,3,*]

[1]*Research Center for Fusion Energy Science and Technology, China Academy of Engineering Physics, Beijing 100088, People's Republic of China*

[2]*Institute of Applied Physics and Computational Mathematics, Beijing 100088, People's Republic of China*

[3]*Center for Applied Physics and Technology, Peking University, Beijing 100871, People's Republic of China*

(Received 30 December 2014; revised manuscript received 18 March 2015; published 14 September 2015)

The problem of electron-ion temperature relaxation in beryllium plasma at various densities (0.185–18.5 g/cm$^3$) and temperatures [(1.0–8)$\times 10^3$ eV] is investigated by using the generalized Lenard-Balescu theory. We consider the correlation effects between electrons and ions via classical and quantum static local field corrections. The numerical results show that the electron-ion pair distribution function at the origin approaches the maximum when the electron-electron coupling parameter equals unity. The classical result of the Coulomb logarithm is in agreement with the quantum result in both the weak ($\Gamma_{ee} < 10^{-2}$) and strong ($\Gamma_{ee} > 1$) electron-electron coupling ranges, whereas it deviates from the quantum result at intermediate values of the coupling parameter ($10^{-2} < \Gamma_{ee} < 1$). We find that with increasing density of Be, the Coulomb logarithm will decrease and the corresponding relaxation rate $\nu_{ie}$ will increase. In addition, a simple fitting law $\nu_{ie}/\nu_{ie}^{(0)} = a(\rho_{\rm Be}/\rho_0)^b$ is determined, where $\nu_{ie}^{(0)}$ is the relaxation rate corresponding to the normal metal density of Be and $\rho_0$, $a$, and $b$ are the fitting parameters related to the temperature and the degree of ionization $\langle Z\rangle$ of the system. Our results are expected to be useful for future inertial confinement fusion experiments involving Be plasma.

DOI: 10.1103/PhysRevE.92.033103 PACS number(s): 52.25.Kn, 52.27.Gr, 52.25.Gj, 05.30.Fk

## I. INTRODUCTION

In order to realize the ignition and high-energy gain in inertial confinement fusion (ICF) [1–10], much effort has been devoted to investigating the physical properties involved in ICF. The temperature relaxation rate is one of various quantities that need to be systematically studied for many aspects of ICF research because the problem of temperature relaxation between electrons and ions in hot dense plasmas is of considerable significance for understanding and controlling the implosion dynamics to ensure successful ignition in ICF. So far, much progress on the temperature relaxations happening in plasmas has been made. Recently, a method of determining coupled-mode temperature relaxation rates via dynamical local field corrections (LFCs) [11–13] has been employed to simulate energy loss in dense hydrogen plasmas by considering particle screening, electron degeneracy, and correlations between electrons and ions. This approach could be regarded as a generalization of the Fermi golden rule [14] and the Lenard-Balescu theory [15], in which the dynamics of electrons and of ions are treated independently. Moreover, molecular dynamics simulations of electron-ion temperature relaxation in a classical Coulomb plasma [16,17] have shown that for weak-coupling parameters, the simulated Coulomb logarithm (CL) agrees with the models developed by Brown *et al.* [18] and by Kihara and Aono [19]. In particular, in Ref. [17] an extensive theoretical analysis using the generalized Lenard-Balescu (GLB) theory was also performed, which includes both the quantum dielectric response together with the bare Coulomb potential and the classical dielectric response together with the statistic potentials. Their results [17] suggested that, compared with molecular dynamics simulations, for hydrogen plasma, GLB calculations in the presence of static LFCs may be worse than GLB calculations in the absence of LFCs.

Furthermore, it is important that the ablator in ICF should be symmetrically imploded since this will result in a small mass of low-density hot fuel at the center surrounded by a larger mass of high-density low-temperature fuel [1,2,20]. Deuterium-tritium (DT) fuel is of primary importance and interest in various kinds of capsules and has been intensively studied. In addition, beryllium is also of interest in ICF due to its appearance in the ablator of the DT capsule and it was suggested that using ions with atomic number $Z > 1$ could be advantageous because of their higher stopping power compared with protons [20–22]. During the ICF implosion process, the complex compression, laser absorption, and instability of the fuel-ablator interface inevitably introduce prominent mixing between DT and Be. As a result, a complete understanding on the physical properties of the warm dense plasma of Be is prerequisite for the ICF design [21,23–26]. For example, the equation of states and electronic transport properties of warm dense Be for densities from 4.0 to 6.0 g/cm$^3$ and temperatures from 1.0 to 10.0 eV have been studied by employing the quantum molecular dynamics simulations [25] and the principal Hugoniot curve is in agreement with underground nuclear explosive and high-power laser experimental results up to ~20 Mbars [23]. However, we have found there is few exhaustive reports on the electron-ion temperature relaxation in Be plasma.

Owing to the importance from the perspective of both basis physics and potential applications of Be in the fields of ICF, it is interesting and timely to provide a theoretical analysis of the electron-ion temperature relaxation of Be plasma. Therefore, for this aspect, we present in this paper a theoretical investigation of the problem of electron-ion temperature relaxation

*Corresponding author: zhang_ping@iapcm.ac.cn

 

in Be plasma at various densities (0.185–18.5 g/cm$^3$) and temperatures [(1.0–8) $\times 10^3$ eV]. In our calculations, (i) the bare Coulomb interaction is assumed; (ii) the mean ionization state of an average ion, i.e., the degree of ionization $\langle Z\rangle$ for Be plasma, is considered; (iii) the correlation effect between electrons and ions is also taken into account consistently via classical and quantum static LFCs; and (iv) electrons are treated as classical and positively (quantum and negatively) charged particles [12], i.e., $Z_e = +1$ ($Z_e = -1$) in the classical like-charge (quantum unlike-charge) Be plasma. Ions are treated as classical particles in both the classical like-charge and quantum unlike-charge cases.

The numerical results show that Be is almost fully ionized when the temperature is higher than 800 eV. With the mean ionization state $\langle Z\rangle$, the density $\rho_{\rm Be}$, and the temperature $T_e$ as inputs, in the classical case (the electrons are assumed to be classical like-charge particles), the classical Ornstein-Zernike equations (COZEs) and a hypernetted-chain closure (HNC) for the correlation functions [27] give self-consistent solutions for the classical static LFCs $G_{\alpha\beta}(k)$ and the corresponding classical pair distribution functions $g_{\alpha\beta}(r)$, with $\alpha,\beta = i,e$ denoting ion and electron species, respectively. In contrast, in the quantum case (the electrons are treated by quantum mechanics), the static quantum electron-ion LFCs and the corresponding quantum pair distribution functions are obtained by considering a cusp-condition approximation. Our quantum results show that the electron-ion pair distribution function at the origin $g_{ie}(r = 0)$, which is the limitation of the quantum electron-ion LFCs at large momentum, approaches the maximum when the dimensionless electron-electron coupling parameter $\Gamma_{ee} = e^2/a_e T_e$ [$a_e = (3/4\pi n_e)^{1/3}$ being the mean interparticle distance] is equal to unity. Furthermore, we find that the classical result of the CL is in agreement with the quantum result in the weak ($\Gamma_{ee} < 10^{-2}$) and strong ($\Gamma_{ee} > 1$) electron-electron coupling range, while it deviates from the quantum result at intermediate values of the coupling parameter ($10^{-2} < \Gamma_{ee} < 1$). In addition, the numerical simulations imply that with increasing density of Be, the CL will decrease and the corresponding relaxation rate $\nu_{ie}$ will increase. A simple fitting law $\nu_{ie}/\nu_{ie}^{(0)} = a(\rho_{\rm Be}/\rho_0)^b$ is also found, where $\nu_{ie}^{(0)}$ is the relaxation rate corresponding to the normal metal density of Be $\rho_0$ and $a$ and $b$ are the dimensionless fitting parameters related to the temperature and the degree of ionization $\langle Z\rangle$ of the system.

The paper is organized as follows. In Sec. II we introduce briefly the main scheme of the GLB theory that we apply to the problem. In Sec. III we show and analyze the results of calculations for several cases of interest. In Sec. IV we summarize the results of this work.

## II. METHOD OF CALCULATION

In the present work we employ the GLB theory proposed in Refs. [12,17], in which the time rates of change of the species temperatures are related to ensemble averages of products of density fluctuations. In the Fourier space, it is explicitly expressed as

$$\frac{dT_\alpha}{dt} = \frac{2}{3n_\alpha V}\sum_{\boldsymbol{k}}\int_0^\infty d\omega\omega v_{\alpha\beta}(\boldsymbol{k})A_{\alpha\beta}(\boldsymbol{k},\omega), \tag{1}$$

where $n_\alpha$ is the number density of particles of species $\alpha$, $V$ is the volume of the system, and $v_{\alpha\beta}(\boldsymbol{k}) = \frac{4\pi\langle Z_\alpha\rangle\langle Z_\beta\rangle e^2}{k^2}$ denotes the Fourier transform of the two-body Coulomb interaction between particles of species $\alpha$ and particles of species $\beta$, with $\langle Z_\alpha\rangle$ and $\langle Z_\beta\rangle$ being the mean ionization states of an average particle of species $\alpha$ and $\beta$, respectively. Here

$$A_{\alpha\beta}(\boldsymbol{k},\omega) = {\rm Im}\langle\delta n_\alpha(\boldsymbol{k},\omega)\delta n_\beta(-\boldsymbol{k},-\omega)\rangle \tag{2}$$

is the imaginary part of the ensemble averages of products of density fluctuations, where $\delta n_\alpha(\boldsymbol{k},\omega)$ is the Fourier transform of the density fluctuations in the presence of interparticle interactions, generally expressed as [27]

$$\delta n_\alpha(\boldsymbol{k},\omega) = \delta n_\alpha^{(s)}(\boldsymbol{k},\omega) + \chi_\alpha^0(\boldsymbol{k},\omega) \times\sum_\beta u_{\alpha\beta}(\boldsymbol{k},\omega)\delta n_\beta(\boldsymbol{k},\omega). \tag{3}$$

In Eq. (3) $\delta n_\alpha^{(s)}(\boldsymbol{k},\omega)$ is the spontaneous fluctuation, $\chi_\alpha^0(\boldsymbol{k},\omega)$ is the free-particle linear polarizability, and

$$u_{\alpha\beta}(\boldsymbol{k},\omega) = v_{\alpha\beta}(\boldsymbol{k})[1 - G_{\alpha\beta}(\boldsymbol{k},\omega)] \tag{4}$$

is the local effective potential with $G_{\alpha\beta}(\boldsymbol{k},\omega)$ being the dynamical LFC. It is well known from the fluctuation-dissipation theorem that the ensemble average of products of the spontaneous density fluctuations could be written as

$$\left\langle\delta n_\alpha^{(s)}(\boldsymbol{k},\omega)\delta n_\beta^{(s)}(-\boldsymbol{k},\omega')\right\rangle = -4\pi\hbar V\delta_{\alpha\beta}\delta(\omega+\omega') \times N\left(\frac{\hbar\omega}{T_\alpha}\right){\rm Im}\,\chi_\alpha^0(k,\omega), \tag{5}$$

where $N(x) = \frac{1}{1-e^{-x}}$ for quantum particles and $N(x) = \frac{1}{x}$ for classical particles. Correspondingly, for instance, one could easily get the time rates of change of the ionic temperature [12,17]

$$\frac{dT_i}{dt} = -\frac{\hbar}{3\pi^3 n_i}\int_0^\infty dkk^2\int_0^\infty d\omega\omega\left[\frac{v_{ie}(k)}{D(k,\omega)}\right]^2 \times\Delta N(k,\omega)[1 - G_{ie}(k,\omega)]\,{\rm Im}\,\chi_i^0(k,\omega)\,{\rm Im}\,\chi_e^0(k,\omega), \tag{6}$$

where $\Delta N(k,\omega) = N(\frac{\hbar\omega}{T_i}) - N(\frac{\hbar\omega}{T_e})$ and

$$D(k,\omega) = \left[1 - u_{ee}\chi_e^0\right]\left[1 - u_{ii}\chi_i^0\right] - u_{ei}u_{ie}\chi_e^0\chi_i^0 \tag{7}$$

essentially denotes the plasma dielectric function.

As discussed in Ref. [12], by considering $m_i T_e \gg m_e T_i$ and the $f$-sum rule for the $\omega$ integral, Eq. (6) can be further simplified to a Landau-Spitzer form [28,29]

$$\frac{dT_i}{dt} = -\nu_{ie}(T_i - T_e), \tag{8}$$

where

$$\nu_{ie} = \nu_0\ln\Lambda(T_i - T_e) \tag{9}$$

is the relaxation rate with $\nu_0 = \frac{8n_e\langle Z\rangle^2 e^4\sqrt{2\pi m_e m_i}}{3(m_i T_e)^{3/2}}$, $m_e$ and $m_i$ being the mass of the electron and ion, respectively, and

$$\ln\Lambda = \int_0^\infty dkF(k) \tag{10}$$

being the CL. Here we define the dimensionless $k$ integrand of the CL as

$$F(k) = \frac{1 - G_{ie}(k)}{k|\epsilon_e(k,0)|^2} f(k/2). \quad (11)$$

To make the problem simple and feasible, we have assumed the static LFC approximation $G_{\alpha\beta}(k,\omega) = G_{\alpha\beta}(k)$ in the following calculations and

$$\epsilon_e(k,0) = 1 - u_{ee}(k,0)\chi_e^0(k,0) \quad (12)$$

is the static electronic dielectric function. If the electrons are treated as classical particles, $f(k/2) = 1$ and $\chi_e^0(k,0) = -\frac{n_e}{T_e}$ in Eq. (11); if the electrons are treated as quantum particles,

$$f(k/2) = \frac{1}{4}\frac{3\sqrt{\pi}\Theta^{3/2}}{1 + \exp\left[\left(k^2/4k_F^2 - \mu/\varepsilon_F\right)/\Theta\right]}, \quad (13)$$

$$\chi_e^0(k,0) = \frac{\eta}{k}\int_0^\infty dy \frac{y \ln|(k/2k_F - y)/(k/2k_F + y)|}{1 + \exp[y^2/\Theta - \mu/T_e]}, \quad (14)$$

where $\eta = m_e k_F^2/(\pi\hbar)^2$ and $\Theta = T_e/\varepsilon_F$ is the degeneracy parameter with $\varepsilon_F = (\hbar k_F)^2/2m_e$ and $k_F = (3\pi^2 n_e)^{1/3}$ being the electronic Fermi energy and momentum, respectively. In addition, we point out that throughout this work the ions are assumed to be classical particles, which is a reasonable approximation. Notice that although the effect of the coupled mode reduces the temperature relaxation rate for higher $\langle Z\rangle$ and lower electron temperature [30], Eqs. (10) and (11) should be reasonable for Be plasma since the ion acoustic modes might not exist for lower charges. Here $\langle Z\rangle = 2$ for temperature $T < 10$ eV and $\langle Z\rangle = 4$ for the highest temperature.

From the above equations we can see that to obtain the CL and the relaxation rate $\nu_{ie}$, one needs to get the LFCs $G_{\alpha\beta}(k)$. Here we choose to solve the LFCs by considering the pair distribution functions $g_{\alpha\beta}(r)$, the conditional probability of finding a particle $\beta$ between $r$ and $r + dr$ away from a particle of species $\alpha$. This is because the static structure factor, which is defined as $S_{\alpha\beta}(k) = \frac{1}{V\sqrt{n_\alpha n_\beta}}\langle\delta n_\alpha(\boldsymbol{k})\delta n_\beta(-\boldsymbol{k})\rangle$, connects $G_{\alpha\beta}(k)$ to $g_{\alpha\beta}(r)$ via Eqs. (3)–(5) and the relationship

$$S_{\alpha\beta}(k) = \delta_{\alpha\beta} + \frac{\sqrt{n_\alpha n_\beta}}{2\pi^2 k}\int_0^\infty dr\, r\sin(kr)[g_{\alpha\beta}(r) - 1]. \quad (15)$$

For the classical case, we focus on the COZE [27] in Fourier space

$$g_{\alpha\beta}(k) = 1 + c_{\alpha\beta}(k) + \sum_\gamma n_\gamma c_{\alpha\gamma}(k)[g_{\gamma\beta}(k) - 1] \quad (16)$$

and the correlated HNC in real space

$$g_{\alpha\beta}(r) = \exp\left[-\frac{v_{\alpha\beta}(r)}{T} + g_{\alpha\beta}(r) - 1 - c_{\alpha\beta}(r)\right], \quad (17)$$

where $c_{\alpha\beta}(k) = -v_{\alpha\beta}(k)[1 - G_{\alpha\beta}(k)]/T$ is the direct correction function, $c_{\alpha\beta}(r) = \frac{1}{2\pi^2 r}\int_0^\infty dk\, k\sin(kr)c_{\alpha\beta}(k)$, and $v_{\alpha\beta}(r) = \frac{\langle Z_\alpha\rangle\langle Z_\beta\rangle e^2}{r}$ is the bare Coulomb interaction. For the quantum case (electrons are treated by the quantum mechanics), the quantum Ornstein-Zernike equations and a hypernetted-chain-like closure for the correlation functions could be solved iteratively to obtain the LFCs (see, for example, Ref. [31]). Alternatively, the quantum electron-ion LFC could also be approximated as [32]

$$G_{ie}(k) = \frac{(1-\alpha)[\varphi(k) - 1]}{(1-\alpha)\varphi(k) + \alpha - \chi_e^0(k,0)u_{ee}(k,0)}, \quad (18)$$

where $\varphi(k) = \frac{\chi_e^0(k,0)}{\chi_e^0(0,0)}$, with $\chi_e^0(0,0) = -\frac{\eta}{k_F}\int_0^\infty \frac{dy}{1+\exp[y^2/\Theta - \mu/T_e]}$, and the parameter $\alpha$ is restricted to satisfy $0 \leqslant \alpha \leqslant 1$ and is determined by the cusp condition on the electron-ion structure factor $S_{ie}(k)$,

$$\int_0^\infty dk k^2 S_{ie}(k) = \xi \lim_{k\to\infty}[k^4 S_{ie}(k)] - 2\pi^2\sqrt{n_e n_i}, \quad (19)$$

with $\xi = \frac{\pi\hbar^2}{8\langle Z\rangle m_e e^2}$. Notice that the structure factor $S_{ie}(k)$ in Eq. (19) could be reduced to the result of the linear-response theory at the small-$k$ limit regardless of $\alpha$, i.e., it satisfies the compressibility sum rule [32].

## III. RESULTS AND DISCUSSION

Before discussing the electron-ion temperature relaxation in Be plasma for densities from 0.185 to 18.5 g/cm$^3$ and temperatures from 1.0 to $8 \times 10^3$ eV, let us first discuss the mean ionization state of an average ion $\langle Z\rangle$ for Be plasma. Numerical calculations based on two different models, a detailed configuration accounting model [33,34] and an average-atom model [35], have been performed. The effect of pressure ionization is considered in both models. The results show that the degrees of ionization for Be based on these two models are almost identical to each other and typical results of the mean ionization state $\langle Z\rangle$ for three different densities obtained by a detailed configuration accounting model are presented in Fig. 1(a). The main idea of the detailed configuration accounting model is briefly introduced in the Appendix. In addition, the results obtained here are also close to with those obtained by Perrot in Ref. [36]. For example, Perrot showed that $\langle Z\rangle = 2.0165$, 2.1405, and 3.3127 in Be plasma with $T_e = 15$, 30, and 100 eV and $\rho_{\rm Be} \approx 6.0$g/cm$^3$, while the detailed configuration accounting model used here gives $\langle Z\rangle = 2.012$, 2.0775, and 3.068 in Be plasma with the same temperatures and density. The mean ionization state for Be is $\langle Z\rangle = 2$ when the temperature is less than 10 eV and it is almost fully ionized ($\langle Z\rangle > 3.9$) when the temperature is larger than 800 eV. Correspondingly, the uniform number density of electrons $n_e$, which is shown in Fig. 1(b), and the

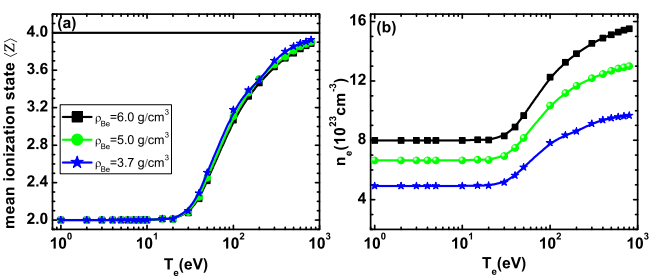


FIG. 1. (Color online) (a) Mean ionization state $\langle Z\rangle$ of an average ion and (b) number densities of electrons as functions of temperature of Be at densities of $\rho_{\rm Be} = 3.7$, 5.0, and 6.0 g/cm$^3$.

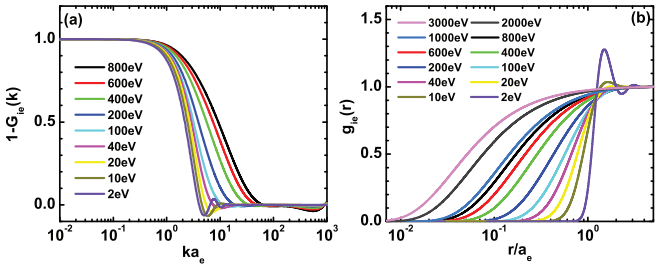


FIG. 2. (Color online) (a) Electron-ion LFC $1 - G_{ie}(k)$ as a function of $ka_e$ and (b) electron-ion pair distribution function $g_{ie}(r)$ as a function of $r/a_e$ for classical like-charged Be at $\rho_{\mathrm{Be}} = 6.0\ \mathrm{g/cm^3}$ and for various temperatures. In the calculations, the mean ionization state of Be plasma shown in Fig. 1 was used.

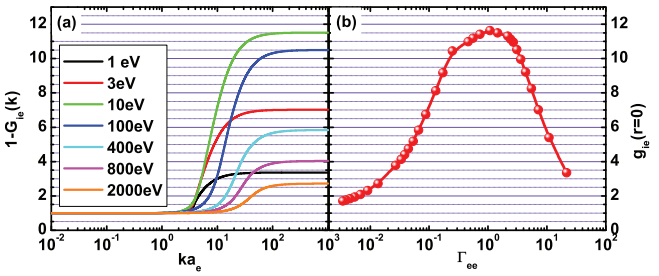


FIG. 3. (Color online) (a) Electron-ion LFC $1 - G_{ie}(k)$ as a function of $ka_e$ and (b) electron-ion pair distribution function at the origin $g_{ie}(r = 0)$ as a function of the Coulomb coupling parameter $\Gamma_{ee}$ for real Be plasma with quantum negative electrons with various temperatures. Other parameters are the same as those in Fig. 2.

electron chemical potential $\mu_e$ (not shown here for briefness) are given by the charge neutrality condition

$$\langle Z\rangle n_i = n_e = \frac{\sqrt{2}}{\pi^2\hbar^3}(m_e T_e)^{3/2} I_{1/2}(\mu_e), \tag{20}$$

where $I_{1/2}(\mu_e)$ is the Fermi integral of index 1/2. Taking the density of Be $\rho_{\mathrm{Be}} = 6.0\ \mathrm{g/cm^3}$ as an instance, we find the number density of electrons is $n_e \approx 8.0 \times 10^{23}\ \mathrm{cm^{-3}}$ when the temperature is less than 10 eV and it gradually increases to $n_e \approx 1.6 \times 10^{24}\ \mathrm{cm^{-3}}$ with increasing temperature to be higher than 800 eV [see the black squares in Fig. 1(b)]. However, the corresponding coupling parameter $\Gamma_{ee}$ decreases with increasing temperature (not shown here).

In the following calculations for the relaxation rate, the mean ionization state $\langle Z\rangle$ and the number density of electrons $n_e$ obtained here are used. It is clear that the temperature relaxation between electrons and ions depends not only on the temperature of the plasma but also on the density of each species in the plasma. Therefore, we study the temperature dependence of the LFC, the pair distribution function, the CL, and the relaxation rate at a fixed density of Be plasma and thus $\rho_{\mathrm{Be}} = 6.0\ \mathrm{g/cm^3}$ is chosen as an example. Under this density condition, the electron-electron coupling parameter $\Gamma_{ee} = 0.0034$–$21.56$ when the temperature changes from 1.0 to $8 \times 10^3$ eV.

In Fig. 2 we exhibit the classical LFC and the corresponding pair distribution function for various values of temperature obtained by self-consistently solving the COZE and HNC, in which the electrons are assumed to be classical and like-charge particles ($Z_e = +1$). We can see from Fig. 2(a) that the classical LFC $1 - G_{ie}(k)$ vanishes at high momentum $k$, which is a reasonable result of the short-range correlations. We also find from the numerical calculations, for each temperature $T_e$, $1 - G_{ie}(k) = 1/2$ at momentum $k = 1/r_L$, where $r_L = e^2/T_e$ is the Landau length, i.e., the appropriate effective $b_{\min}$ of the CL. This result is consistent with previous calculations performed on hydrogen plasma [12]. The classical electron-ion pair distribution function $g_{ie}(r)$ increases to unity from zero without oscillations when the temperature is high enough (corresponding to weak coupling), while $g_{ie}(r)$ will oscillate out of the electron sphere radius several times when the temperature becomes low (<10 eV). For example, the first two peaks of $g_{ie}(r)$ can be clearly observed when the temperature $T_e = 2$ eV [see the purple line in Fig. 2(b)]. The ion-ion and electron-election pair distribution functions could also be obtained self-consistently, which are not shown here for briefness.

In the classical case, as suggested in Ref. [12], the GLB model will diverge when the electrons are treated as classical negatively charged particles ($Z_e = -1$) even if the static LFC is taken into account in the calculations. In contrast, the GLB model will converge if the negatively charged electrons are treated by quantum mechanics. The typical results for the quantum static LFC obtained from the cusp-condition approximation are presented in Fig. 3(a). Differing from the classical case, the quantum LFC $1 - G_{ie}(k) \geqslant 1$ and its limitation at large momentum $k$ is the value of the electron-ion pair distribution function at the origin $g_{ie}(r = 0)$, which is shown in Fig. 3(b) as a function of the coupling parameter $\Gamma_{ee}$. The correlation effect becomes important in the calculation of the CL when the quantum LFC at large momentum $[\lim_{k\to\infty} 1 - G_{ie}(k)]$ significantly increases and the value of the CL in the presence of the LFC becomes larger than the value obtained from the models ignoring LFC $[G_{\alpha\beta}(k) = 0]$. This is why we consider the quantum LFC in our calculations. Furthermore, Fig. 3(b) shows that $g_{ie}(r = 0)$ approaches a maximum when the coupling parameter $\Gamma_{ee} = 1$ and $g_{ie}(r = 0)$ decreases to unity in the weak- or strong-coupling regime (note that $\lim_{k\to\infty}[1 - G_{ie}(k)] = g_{ie}(r = 0)$, which indicates $g_{ie}(r = 0) \geqslant 1$).

In addition, we have also calculated the quantum electron-ion pair distribution function $g_{ie}(r)$. Selected results of $g_{ie}(r)$ as a function of $r/a_e$ are plotted in Fig. 4(a). Different from the classical case [Fig. 2(b)], the quantum pair distribution function $g_{ie}(r) \geqslant 1$ and decreases to unity at large distance. Through the Fourier transform $S_{ie}(k) = \frac{\sqrt{n_i n_e}}{2\pi^2 k}\int_0^\infty dr\, r \sin(kr)[g_{ie}(r) - 1]$, the behavior of $g_{ie}(r)$ could also be observed from the static structure factor $S_{ie}(k)$, which reveals the influence of electron-ion collisions and the electron accumulation at the sites of the ions in momentum space. The corresponding $S_{ie}(k)$ obtained using the cusp-condition approximation as a function of $ka_e$ is shown in Fig. 4(b). It is clear that $S_{ie}(k)$ tends to vanish at large momentum and approaches a finite nonzero value at small momentum ($k \to 0$); another feature of Fig. 4(b) is the manner in which $S_{ie}(k)$ approaches zero more quickly for higher temperature.

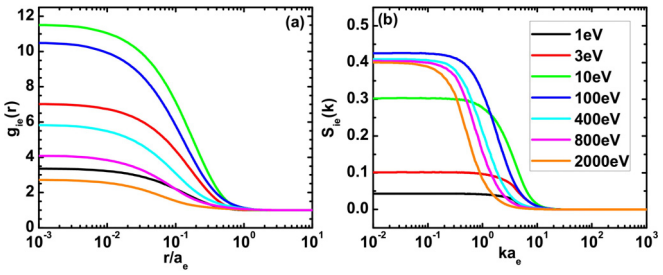


FIG. 4. (Color online) (a) Electron-ion pari-distribution function $g_{ie}(r)$ as a function of $r/a_e$ and (b) electron-ion static structure factor $S_{ie}(k)$ as a function of $ka_e$ for real Be with quantum negative electrons with various temperatures. Other parameters are the same as those in Fig. 2.

This is because the plasma becomes more weakly coupled as the temperature increases.

After obtaining the LFC, one could easily get the CL by using Eqs. (10) and (11). In Fig. 5(a) we show the results for $kF(k)$ versus $ka_e$ obtained using the GLB model for various values of temperature at a definite density of $\rho_{\rm Be} = 6.0{\rm g/cm}^3$. From Fig. 5(a) we can observe that $kF(k)$ approaches the maximum value almost at $ka_e \approx 3$, which is insensitive to the density and temperature of plasma, and $F(k)$ decreases to zero gradually (quickly) with increasing (decreasing) momentum $k$ from the value corresponding to max$[kF(k)]$ because of the remarkable quantum diffraction in the limit of large momentum [the sharp increase in $\epsilon_e(k,0)$ in the limit of small momentum]. Furthermore, Fig. 5(a) shows that the value of $kF(k)$ increases with increasing temperature and max$[kF(k)] \to 1$ in the high-temperature (corresponding to weak-coupling) limit, which is similar to the results for H plasma shown in Ref. [17]. In this way, we can see that the GLB model could be approximated by the Landau-Spitzer model [17,28,29] in weakly coupled plasma since the Landau-Spitzer model suggests $\ln\Lambda = \int F(k)dk = \int_{b_{\rm max}^{-1}}^{b_{\rm min}^{-1}} \frac{dk}{k} = \ln(\frac{b_{\rm max}}{b_{\rm min}})$, where $b_{\rm max} = \lambda_{\rm De}$ and $b_{\rm min} \approx 0.778\lambda_{\rm th}$ are the maximum and minimum impact parameters, respectively,

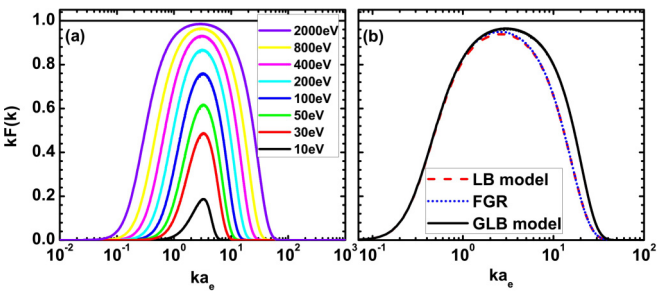


FIG. 5. (Color online) (a) Plot of $kF(k)$ [see the text for the definition in Eq. (11)] vs $ka_e$ for various electronic temperatures of Be plasma obtained using the GLB model with local field corrections $G_{\alpha\beta}$. (b) Plot of $kF(k)$ vs $ka_e$ for $T_e = 800$ eV for Be plasma. The results are obtained using the GLB model with the LFC $G_{\alpha\beta} \neq 0$ (black line), the Fermi golden rule with $G_{ie} = 0$ and $G_{ee}$ approximated by the Vashista-Singwi form (blue dotted line), and the LB model with $G_{\alpha\beta} = 0$ (red dashed line). Other parameters are the same as those in Fig. 2.

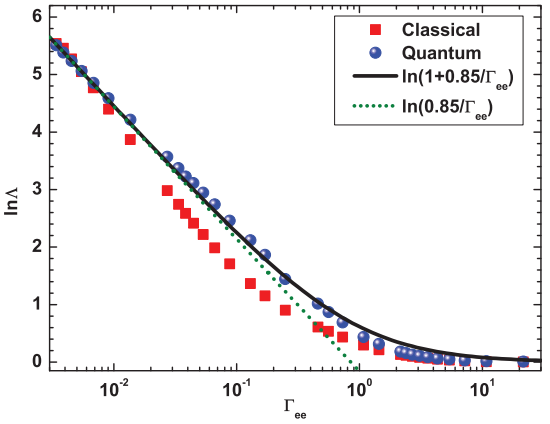


FIG. 6. (Color online) The CL vs plasma parameter $\Gamma_{ee}$ for dense Be. The red squares are for the classical like-charge results obtained using COZEs and the HNC and the blue dots are for the quantum results obtained using the cusp-condition approximation. The black curved line is a fit to the quantum data and the green dotted line is a fit to the result in the weak-coupling regime. Other parameters are the same as those in Fig. 2.

with $\lambda_{\rm De} = (T_e/4\pi n_e e^2)^{1/2}$ being the electron Debye wavelength and $\lambda_{\rm th} = (\hbar^2/m_e T_e)^{1/2}$ the electron thermal de Broglie wavelength. For comparison, in Fig. 5(b) we additionally show the results of $kF(k)$ for $T_e = 800$ eV obtained using the Fermi golden rule [14] with $G_{ie} = 0$ and $G_{ee}$ approximated by the Vashista-Singwi form (blue dotted line) and the LB model [15] in the absence of the LFC $G_{\alpha\beta} = 0$ (red dashed line). It is clear that the result of $kF(k)$ obtained from the GLB model [17] (black line) is larger than the results obtained from the other two models. In particular, when $ka_e > 3$, the difference is distinguishable due to the remarkable short-range screening and correlation effects between electrons and ions taken into account via the LFC $G_{ie}$. This result reveals that the value of the CL with the LFC should be larger than that without the LFC. We can also see from Fig. 5(b) that the result obtained from the Fermi golden rule is indistinguishable from that of the Lenard-Balescu model.

Substituting the above-obtained LFC into Eq. (10), it is easy to get the CL. Here we point out that in order to obtain a convergent and proper CL for like-charged classical plasma ($Z_e = 1$), large enough distance $r$ and momentum $k$ are chosen and $2^{17}$ points in $r$ and $k$ are set in our numerically self-consistent iterations for solving the COZE and HNC [17]. The result of $\ln\Lambda$ for Be plasma at a density of $\rho_{\rm Be} = 6.0$ g/cm$^3$ and various temperatures (from 1 to $8 \times 10^3$ eV) is shown in Fig. 6 as a function of the plasma coupling parameter $\Gamma_{ee}$, in which the red squares present the result for like-charged classical plasma and the blue dots show the result for oppositely charged quantum plasma. It is obvious that in the strong-coupling case ($\Gamma_{ee} > 1$), the classical result of the CL is in agreement with the quantum result. This is reasonable and results from the fact that the effective $b_{\rm min} = \lambda_L$ (the Landau length $\lambda_L = \langle Z\rangle e^2/T_e$) is sure to be larger than the electron thermal de Broglie length $\lambda_{\rm th}$ at low enough temperature. Furthermore, the classical result of the CL is also in agreement with the quantum result in the weak electron-electron coupling

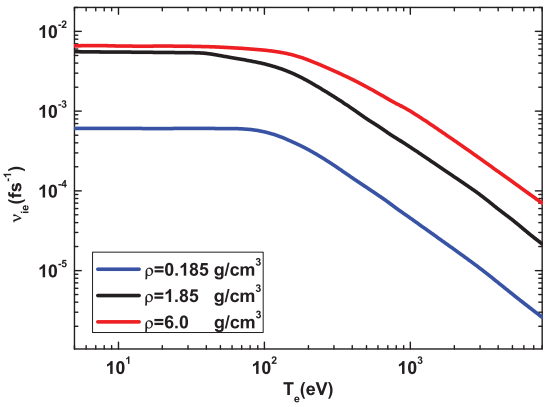


FIG. 7. (Color online) Relaxation rates $\nu_{ie}$ for Be plasma at densities 0.185 g/cm$^3$ (blue), 1.85 g/cm$^3$ (black), and 6.0 g/cm$^3$ (red) obtained using the GLB model with the quantum LFC $G_{\alpha\beta}$. Other parameters are the same as those in Fig. 2.

range ($\Gamma_{ee} < 10^{-2}$). There are two reasons for this agreement. First, the GLB model (both the classical case and the quantum case) is reduced to the Landau-Spitzer model and the Brown *et al.* model in the weak-coupling range [17], which recover the same result even in the quantum limit $\lambda_L < \lambda_{\rm th}$ for much higher temperature [18,28,29] ($\lambda_L \leqslant \lambda_{\rm th}$ with $\langle Z\rangle \sim 4$ for $T_e \geqslant 1$ keV). Second, the quantum statistics effect could be reduced to classical statistics at high temperature, namely, the Fermi distribution is reduced to the Maxwellian distribution. A notable difference between the quantum result and the classical result is observed for intermediate values of $\Gamma_{ee}$. This may be due to the partial electron degeneracy in this coupling regime, which is included in the static electronic dielectric function [see Eqs. (12)–(14)]. Indeed, the classical result of the CL shown here cannot predict the temperature equilibration of a real Be plasma since the physics is ignored in the classical like-charge pure-Coulomb cases [17] and therefore we focus on the quantum result in the following discussion. The quantum result of $\ln\Lambda$ could be well fitted by a logarithmic function $\sim\ln(1+0.85/\Gamma_{ee})$ in a wide range of $\Gamma_{ee}$ (see the black curved line in Fig. 6) and in the weakly coupled regime ($\Gamma_{ee} < 0.1$) it could be fitted also by $\sim\ln(0.85/\Gamma_{ee})$ (see the green dotted line in Fig. 6). We have also numerically checked that our result is consistent with the Landau-Spitzer result and the Brown *et al.* result in the weakly coupled limitation.

The temperature relaxation rate $\nu_{ie}$ between quantum oppositely charged electrons and classical ions in Be plasma at density $\rho_{\rm Be} = 6.0$ g/cm$^3$ is shown by a red curve in Fig. 7 as a function of electron temperature $T_e$. Furthermore, for comparison, we have also calculated $\nu_{ie}$ at normal metal density $\rho_{\rm Be} = 1.85$ g/cm$^3$ and expanded Be density $\rho_{\rm Be} = 0.185$ g/cm$^3$ (see the black and blue curves in Fig. 7). In all of the calculations, the mean ionization state $\langle Z\rangle$ is considered and the Fermi energy $\varepsilon_F$ is not a constant due to partial ionization at low temperatures. There are at least two points in Fig. 7 that need to be noticed: (i) It is clear that lower density gives a lower relaxation rate and (ii) similar to hydrogen plasma, $\nu_{ie}$ keeps nearly invariant when the temperature is smaller than 100 eV since $\nu_0$ is proportional to $T_e^{-3/2}$, which is comparable to $\ln\Lambda$ scaling like $T_e^{3/2}$ at small $T_e$. In contrast, $\nu_{ie}$

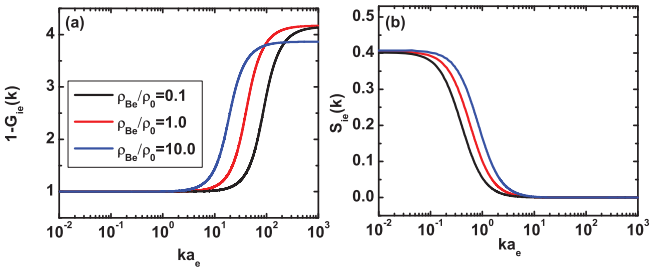


FIG. 8. (Color online) (a) Electron-ion LFC $1 - G_{ie}(k)$ and (b) electron-ion static structure factor $S_{ie}(k)$ vs $ka_e$ for real Be with quantum negative electrons at $\rho_{\rm Be}/\rho_0 = 0.1$, 1.0, and 10.0 for $T_e =$ 800 eV. Here $\rho_0$ is the normal metal density of Be.

decreases when the temperature is higher than 100 eV because the correlation effect becomes weak at high temperatures. Compared with previous studies on the hydrogen plasma with a similar electron number density [12], the temperature relaxation rate $\nu_{ie}$ for Be plasma considered herein is smaller than that for hydrogen plasma because of the heavier ions in Be plasma.

In the above calculations we focused on the Be plasma at density $\rho_{\rm Be} = 6.0$ g/cm$^3$. Now let us turn to study the response of relaxation rate to the density of Be plasma at a fixed temperature. Here $T_e = 800$ eV is chosen as an example and the density of Be is changed from $0.1\rho_0$ to $10\rho_0$ in the following discussion, where $\rho_0 = 1.85$ g/cm$^3$ is the normal metal density of Be. The corresponding electron-electron coupling parameter $\Gamma_{ee}$ changes from 0.0106 to 0.0484. The numerical calculations show that the LFC and structure factor are insensitive to the density of plasma. For instance, $1 - G_{ie}(k)$ and $S_{ie}(k)$ as functions of $ka_e$ for Be plasma with quantum electrons at $\rho_{\rm Be}/\rho_0 = 0.1$, 1.0, and 10.0 are shown in Fig. 8, from which we can see that with increasing the density from $0.1\rho_0$ to $10\rho_0$, $\lim_{k\to\infty}[1 - G_{ie}(k)]$ decreases from 4.1505 to 3.8647 and $\lim_{k\to 0} S_{ie}(k) \approx 0.4$. However, $S_{ie}(k)$ approaches zero more quickly for lower density at fixed temperature since plasma becomes more weakly coupled as the density decreases.

Furthermore, we show $kF(k)$ in Fig. 9 as a function of $ka_e$ for various densities of Be plasma at temperature $T_e = 800$ eV. It is obvious that $kF(k) \to 1$ at intermediate momentum $k$ with decreasing density. Correspondingly, the numerical data of $\ln\Lambda$ as a function of $\rho_{\rm Be}/\rho_0$ for different temperatures $T_e = 1$, 100, 800, 2000, and 5000 eV are shown in Fig. 10(a). One can clearly see that the CL $\ln\Lambda$ decreases with increasing density. The falloff in the $\ln\Lambda$ with density could be well fitted by $\ln\Lambda = c(\rho_{\rm Be}/\rho_0)^d$, where $c$ and $d$ are the dimensionless fitting parameters shown in Table I for different temperatures. Since they depend smoothly on density, the parameters $c$ and $d$ may be obtained for other values of $T_e$ by interpolation. However, the electron-ion temperature relaxation rate $\nu_{ie}$ increases with increasing density [see Fig. 10(b)], which could be simply fitted by

$$\nu_{ie}/\nu_{ie}^{(0)} = a(\rho_{\rm Be}/\rho_0)^b, \tag{21}$$

where $\nu_{ie}^{(0)} = 4.5603 \times 10^{-4}$fs$^{-1}$ corresponds to the metal density of Be $\rho_0 = 1.85$ g/cm$^3$ and the fitting parameters $a$

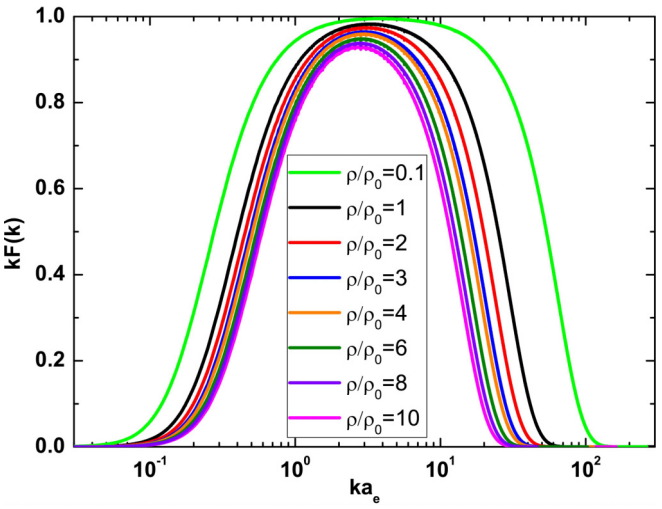


FIG. 9. (Color online) Plot of $kF(k)$ vs $ka_e$ for various densities of Be plasma with temperature $T_e = 800$ eV.

and $b$ are shown in Table I for different temperature values (see also [37]). The parameter $a$ is close to 1.1 and the parameter $b$ smoothly increases from 0.05 to 0.868 for $T_e$ changing from 1 to 5000 eV. Using this fitting function, one can estimate the electron-ion temperature relaxation rate $\nu_{ie}$ at desired densities and temperatures and it may be useful for related ICF experiments in the future.

## IV. CONCLUSION

The electron-ion temperature relaxation in Be plasma at various densities and temperatures was investigated by employing the GLB model, where the correlation effects between electrons and ions were self-consistently included via static LFCs. The effect of the mean ionization state was also included. The COZE and HNC (cusp-condition approximation) were solved to obtain the classical (quantum) static LFC $G_{\alpha\beta}(k)$ and the corresponding classical (quantum) pair distribution functions $g_{\alpha\beta}(r)$. The numerical results showed that the classical result of the CL is in agreement with the quantum result at either weak or strong electron-electron coupling parameters, while it deviates from the quantum result at intermediate values of the coupling parameter. Furthermore, it was found that with increasing the density of Be, the CL will decrease and the corresponding relaxation rate will increase. In addition, a simple increasing law $\nu_{ie}/\nu_{ie}^{(0)} = a(\rho_{\rm Be}/\rho_0)^b$ was determined. There results are expected to be useful for future inertial confinement fusion experiments involving Be plasma.

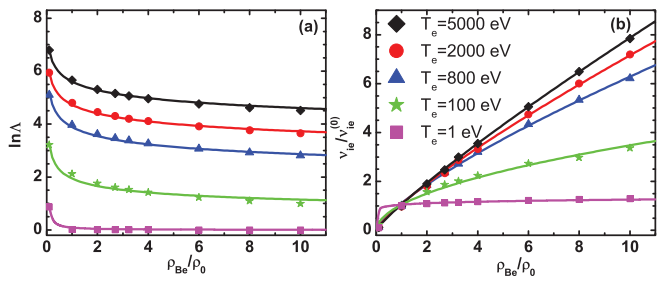


FIG. 10. (Color online) (a) The CL $\ln\Lambda$ and (b) relaxation rate $\nu_{ie}/\nu_{ie}^{(0)}$ vs $\rho_{\rm Be}/\rho_0$ with temperature $T_e = 1$ eV (magenta squares), 100 eV (green stars), 800 eV (blue triangles), 2000 eV (red circles), and 5000 eV (black diamonds). The lines are fits to the numerical data. In the numerical calculations, $\rho_{\rm Be}$ is chosen as 0.185, 1.85, 3.7, 5.0, 6.0, 7.4, 11.1, 14.8, and 18.5 g/cm$^3$. Here $\rho_0 = 1.85$ g/cm$^3$ is the normal metal density of Be.

TABLE I. Fitting parameters $a$ and $b$ ($c$ and $d$) for relaxation rate (CL) as a function of the density of Be at different temperatures.

| $T_e$ (eV) | a | b | c | d |
|---|---|---|---|---|
| 1 | 1.05 | 0.050 | 0.088 | −1.014 |
| 100 | 1.05 | 0.520 | 1.944 | −0.229 |
| 800 | 1.11 | 0.753 | 3.888 | −0.133 |
| 2000 | 1.08 | 0.820 | 4.730 | −0.103 |
| 5000 | 1.07 | 0.868 | 5.605 | −0.085 |


## ACKNOWLEDGMENTS

This work was supported by National Natural Science Foundation of China under Grants No. 11275032, No. 11575032, No. 11205019, No. 11304009, and No. U1530258 and by the Foundation for the Development of Science and Technology of CAEP under Grant No. 2014B0102015. Z.-G.F. was partially supported by the China Postdoctoral Science Foundation under Grant No. 2014T70029.


## APPENDIX: INTRODUCTION OF THE DETAILED CONFIGURATION ACCOUNTING MODEL

By employing a detailed configuration accounting model with the term structures treated by the unresolved transition array model, we have calculated the mean ionization of an average ion $\langle Z\rangle$ for Be plasma. The detailed configuration accounting model is a method consisting of the fully relativistic treatment incorporated with the quantum defect theory to calculate the atomic parameters [33,34]. A huge number of configurations with high principal quantum number are considered in this model. The fraction of incident radiation transmitted through the plasma is written as a decaying exponential function $F(\omega) = \exp[-\gamma(\omega)L]$, where $L$ is the path length traversed by the light through the plasma and $\gamma(\omega)$ is the absorption coefficient, which is expressed as [34]

$$\gamma(\omega) = \sum_i \left[ \sum_{c,c'} N_{i,c}\sigma^{bb}_{i,c,c'}(\omega) + \sum_c N_{i,c}\sigma^{bf}_{i,c}(\omega) \right] + N_e\sigma^{ff}(\omega) \quad \text{(A1)}$$

under the configuration average approximation. Here $i$ is the ionic stage, $N_{i,c}$ ($N_e$) is the number of ions of configuration $c$ (the number of electrons) per unit volume, $\sigma^{bb}_{i,c,c'}(\omega)$ is the bound-bound photoexcitation cross section from configuration $c$ to $c'$, $\sigma^{bf}_{i,c}(\omega)$ is the bound-free photoionization cross section from all subshells of configuration $c$, and $\sigma^{ff}(\omega)$ denotes the free-free absorption cross section. For the local thermodynamic equilibrium plasmas, the charge state distribution and the mean ionization of an average ion $\langle Z\rangle$ can be obtained by

solving the Boltzmann-Saha equation [38]

$$\frac{N_{i+1,c}N_e}{N_{i,c}} = \frac{\mathcal{Z}_e\mathcal{Z}_{i+1}}{\mathcal{Z}_i}e^{-(\phi_i-\Delta\phi_i)/T}, \tag{A2}$$

where $\mathcal{Z}_i$ and $\mathcal{Z}_e$ denote the partition function of ionization stage $i$ and free electrons, respectively, and $\phi_i$ and $\Delta\phi_i$ are the ionization potential and ionization potential depression (the Debye-Hückel model) [39] of ionization stage $i$, respectively. In the detailed configuration accounting model, the self-consistent-field energy-level database is employed to investigate and produce important configurations and thereby the most important configurations are taken into account in solving Boltzmann-Saha equations.


[1] S. Atzeni and J. Meyer-ter-Vehn, *The Physics of Inertial Fusion: Beam Plasma Interaction, Hydrodynamics, Hot Dense Matter*, International Series of Monographs on Physics (Clarendon, Oxford, 2004).

[2] J. D. Lindl, *Inertial Confinement Fusion: The Quest for Ignition and Energy Gain Using Indirect Drive* (Springer, New York, 1998).

[3] J. R. Rygg, F. H. Séguin, C. K. Li, J. A. Frenje, M. J.-E. Manuel, R. D. Petrasso, R. Betti, J. A. Delettrez, O. V. Gotchev, J. P. Knauer *et al.*, Science **319**, 1223 (2008).

[4] P. A. Norreys, Science **327**, 1208 (2010).

[5] S. H. Glenzer, B. J. MacGowan, P. Michel, N. B. Meezan, L. J. Suter, S. N. Dixit, J. L. Kline, G. A. Kyrala, D. K. Bradley, D. A. Callahan *et al.*, Science **327**, 1228 (2010).

[6] C. K. Li, F. H. Séguin, J. A. Frenje, M. Rosenberg, R. D. Petrasso, P. A. Amendt, J. A. Koch, O. L. Landen, H. S. Park, H. F. Robey *et al.*, Science **327**, 1231 (2010).

[7] C. K. Li, F. H. Séguin, J. A. Frenje, M. J. Rosenberg, H. G. Rinderknecht, A. B. Zylstra, R. D. Petrasso, P. A. Amendt, O. L. Landen, A. J. Mackinnon *et al.*, Phys. Rev. Lett. **108**, 025001 (2012).

[8] O. A. Hurricane, D. A. Callahan, D. T. Casey, P. M. Celliers, C. Cerjan, E. L. Dewald, T. R. Dittrich, T. Döppner, D. E. Hinkel, L. F. Berzak Hopkins *et al.*, Nature (London) **506**, 343 (2014).

[9] W. Theobald, A. A. Solodov, C. Stoeckl, K. S. Anderson, F. N. Beg, R. Epstein, G. Fiksel, E. M. Giraldez, V. Yu. Glebov, H. Habara *et al.*, Nat. Commun. **5**, 5785 (2014).

[10] L. Lancia, B. Albertazzi, C. Boniface, A. Grisollet, R. Riquier, F. Chaland, K.-C. Le Thanh, Ph. Mellor, P. Antici, S. Buffechoux *et al.*, Phys. Rev. Lett. **113**, 235001 (2014).

[11] M. W. C. Dharma-wardana, Phys. Rev. Lett. **101**, 035002 (2008).

[12] J. Daligault and G. Dimonte, Phys. Rev. E **79**, 056403 (2009).

[13] M. D. Barriga-Carrasco, Phys. Rev. E **79**, 027401 (2009).

[14] G. Hazak, Z. Zinamon, Y. Rosenfeld, and M. W. C. Dharma-wardana, Phys. Rev. E **64**, 066411 (2001).

[15] D. O. Gericke, J. Phys.: Conf. Ser. **11**, 111 (2005).

[16] G. Dimonte and J. Daligault, Phys. Rev. Lett. **101**, 135001 (2008).

[17] L. X. Benedict, M. P. Surh, J. I. Castor, S. A. Khairallah, H. D. Whitley, D. F. Richards, J. N. Glosli, M. S. Murillo, C. R. Scullard, P. E. Grabowski, D. Michta, and F. R. Graziani, Phys. Rev. E **86**, 046406 (2012).

[18] L. S. Brown, D. L. Preston, and R. L. Singleton, Jr., Phys. Rep. **410**, 237 (2005).

[19] T. Kihara and O. Aono, J. Phys. Soc. Jpn. **18**, 837 (1963).

[20] A. Macchi, M. Borghesi, and M. Passoni, Rev. Mod. Phys. **85**, 751 (2013), and references therein.

[21] J. D. Lindl, P. Amendt, R. L. Berger, S. G. Glendinning, S. H. Glenzer, S. W. Haan, R. L. Kauffman, O. L. Landen, and L. J. Suter, Phys. Plasmas **11**, 339 (2004).

[22] M. H. Key, Phys. Plasmas **14**, 055502 (2007).

[23] C. E. Ragan III, Phys. Rev. A **25**, 3360 (1982).

[24] W. J. Nellis, J. A. Moriarty, A. C. Mitchell, and N. C. Holmes, J. Appl. Phys. **82**, 2225 (1997).

[25] C. Wang, Y. Long, M.-F. Tian, X.-T. He, and P. Zhang, Phys. Rev. E **87**, 043105 (2013).

[26] Z. Wang, Z.-G. Fu, B. He, and P. Zhang, Phys. Plasmas **21**, 072703 (2014).

[27] S. Ichimaru, *Statistical Plasma Physics* (Addison-Wesley, Reading, 1992), Vol. I.

[28] L. D. Landau, Phys. Z. Sowietjunion **10**, 154 (1936) [Sov. Phys. JETP **7**, 203 (1937)].

[29] L. Spitzer, *Physics of Fully Ionized Gases* (Interscience, New York, 1962).

[30] J. Vorberger and D. Gericke, Phys. Plasmas **16**, 082702 (2009).

[31] H. Xu and J.-P. Hansen, Phys. Rev. E **57**, 211 (1998).

[32] K. Nagao, S. A. Bonev, and N. W. Ashcroft, Phys. Rev. B **64**, 224111 (2001).

[33] J. Yan and Z.-Q. Wu, Phys. Rev. E **65**, 066401 (2002).

[34] J. Yan and Y.-B. Qiu, Phys. Rev. E **64**, 056401 (2001).

[35] A. F. Nikiforov and V. G. Novikov, *Quantum-Statistical Models of Hot Dense Matter: Methods for Computation Opacity and Equation of State* (Springer, Berlin, 2000).

[36] F. Perrot, Phys. Rev. E **47**, 570 (1993).

[37] C. M. Lee, L. Kissel, and R. H. Pratt, Phys. Rev. A **13**, 1714 (1976).

[38] R. D. Cowan, *Theory of Atomic Spectra* (University of California Press, Berkeley, 1981).

[39] D. J. Heading, J. S. Wark, G. R. Bennett, and R. W. Lee, J. Quant. Spectrosc. Radiat. Transfer **54**, 167 (1995), and references therein.